Structural, Chemical, and Electronic Properties of Pt/Ni Thin Film Electrodes for Methanol Electrooxidation

Kyung-Won Park, Jong-Ho Choi, and Yung-Eun Sung*

Department of Materials Science & Engineering and Center for Frontier Materials, Kwangju Institute of Science and Technology (K-JIST), Kwangju 500-712, South Korea

Received: January 14, 2003; In Final Form: April 21, 2003

Pt/Ni thin-film electrodes were fabricated by e-beam evaporation of metal layers and rapid thermal annealing (RTA), to achieve alloy formation between the Pt and Ni layers. The structural, chemical, and electronic properties of thin-film electrodes annealed at 200, 300, and 500 °C were classified as follows: Pt-dominant (as-Pt/Ni or 200 °C Pt/Ni), Pt-based (300 °C Pt/Ni), and Ni-dominant (500 °C Pt/Ni). These Pt/Ni thin-film electrodes were matched well with Pt/Ni(3:1), -(1:1), and -(1:3) nanoparticles synthesized by borohydride reduction, for use in methanol electrooxidation in a direct methanol fuel cell. The characteristics of the thin-films and nanoparticles were correlated using X-ray diffraction analysis, Auger electron spectroscopy, X-ray photoelectron spectroscopy, and electrochemical measurements. The modified electronic properties of platinum in Pt/Ni alloy electrodes as well as a higher catalytic activity for methanol electrooxidation could be attributed to the surface and bulk structure of Pt/Ni alloys with a proper composition such as 300 °C Pt/Ni thin-film electrode and Pt/Ni(1:1) nanoparticle. The possibility that electrodes designed by thin-film processing such as by means of an e-beam evaporator and RTA system could be used in a systematic approach to the characterization of alloy nanoparticles is discussed.

Introduction

The excellent catalytic activity of platinum for methanol oxidation, especially, at low temperatures (<80 °C) makes this metal electrocatalyst ideal for use as an anode in direct methanol fuel cells (DMFCs), which are currently of great interest because of a variety of advantages that include high energy density, ease of handling a liquid, and low operating temperatures.[1−6] However, it is well-known that a pure platinum is readily poisoned by CO, a byproduct in methanol electrooxidation, at low temperatures. Accordingly, to enhance its catalytic activity for methanol electrooxidation by eliminating or inhibiting the CO poisoning effect, many efforts have been reported to design and synthesize Pt-based alloy catalysts by alloying platinum with 2nd or 3rd elements on the basis of a bifunctional mechanism, an electronic effect, or an ensemble effect.[7−9]

According to the bifunctional mechanism, anode catalysts in DMFCs have been studied the most intensively. The CO poisoned platinum can be regenerated via the reaction of surface CO with oxygen species associated with elements such as ruthenium and osmium to yield CO_2.[10,11] Smotkin et al. reported on improved methanol electrooxidation catalysts such as PtRu, PtOs, and PtRuOs and confirmed the role of ruthenium and osmium as oxygen sources, consistent with the bifunctional mechanism.[12] Goodenough et al. reported a shift in the Pt 4f peak of a Pt/Ru alloy using X-ray photoelectron spectroscopy (XPS) analysis, showing that some electronic effects can also be involved in ruthenium enhancement.[13] In addition, the electronic properties of Pt/Ni, Pt/Co, and Pt/Fe thin-film electrodes have been confirmed by a d-vacancy shift in XPS.[14] In particular, we found that Pt/Ni and Pt/Ru/Ni nanopaticles showed a shift in the Pt 4f peak in a Pt/Ni-based alloy structure, so-called the electronic effect.[7] Enhanced catalytic activity such as lower onset potential and improved stability in methanol electrooxidation was responsible for the change in the electronic properties of Pt in Pt/Ni alloys. However, overall, the issue of whether the second metal is involved in the modification of the Pt electronic structure remains unclear. Therefore, further progress in fuel cell catalysis, especially on a nanoparticle surface, and further characterization of catalysts are required. Goodman's group described the nature of the metal−metal bond in bimetallic surfaces and perturbations in the electronic, chemical, and catalytic properties in great detail.[15,16] However, to compare various bimetallic surfaces with alloy nanoparticles, the surface structure of bimetallic systems must have structural and electronic properties that are comparable with those of bulk of nanoparticles. Accordingly, we designed Pt/Ni based alloy thin-film electrodes with a variety of structural and electronic properties using an e-beam evaporator for depositing Pt and Ni metal and a rapid thermal annealing system to achieve alloy formation by the intermixing of Pt and Ni film layers. The resulting Pt/Ni thin-film electrodes could be compared and correlated with Pt/Ni nanoparticles of any composition.

Experimental Section

Si and Pt/Ti/Si were used as substrates for the structural analysis and electrochemical measurements, respectively. The electron beam evaporation method was used to deposit Pt/Ni thin metal films. In electron beam evaporation, a focused electron beam with a high intensity was used to vaporize metal source materials such Pt and Ni, which were placed in a small boat. The evaporated atoms travel in all directions and condense on the surface of the substrate located in front of the source material. By placing an evaporation mask and thickness monitor in front of the substrate, the geometry and thickness of the evaporated metal film can be adjusted, thus permitting excellent uniformity to be attained. A commercial e-beam evaporator (PLS

* To whom correspondence should be addressed.

10.1021/jp0340966 CCC: $25.00
Published on Web 05/16/2003

500, Pfeiffer Vacuum) was used for depositing all thin-film layers. The thin-film layer for a fuel electrode was deposited under a background vacuum pressure of 5×10^{-7} Torr. The thicknesses of the bottom and top layers were ~40 nm for Ni and 5−6 nm for Pt. For alloy formation between the metallic layers, rapid thermal annealing (RTA) was performed for 30 s at 200, 300, and 500 °C under flowing N_2 gas. The pyrometer was used in the RTA system, and the annealing temperatures were calibrated on the SiC holder. The temperature overshoots were very small (<3 °C), and steady-state temperatures were reached in 5 s. The samples were not encapsulated in a SiC holder assembly in the RTA chamber.

Structural analyses of Pt-based catalysts were carried out using a Rigaku X-ray diffractometer equipped with a Cu Kα source. To estimate the composition of the platinum alloy thin-film electrodes, the (111) peak was fitted using the Lorentzian/Gaussian function. The composition was determined using Vegard's law. The variation in composition as a function of the depth of the samples was performed by Auger electron spectroscopy (AES) using a PHI 670 Auger microscope with an electron beam of 10 keV and 0.0236 μA, and the base pressure of the system was 10^{-10} Torr. Depth profiling at the sputter rate of 30 Å min^{-1} was carried out to survey the variation in composition at a depth from the surface layer of the thin-film electrode. To analyze and compare the surface chemical states of the samples, X-ray photoelectron spectroscopy (XPS) was carried out using a VG Scientific (ESCALAB 200R) photoelectron spectrometer. The X-ray source was Al Kα with 1486.6 eV operating at 15 kV and 300 W. The base pressure of the system was 10^{-10} Torr. The XPS core-level spectra were fitted to the Doniach−Sunjic line shape convoluted by a Gaussian contribution taking into account the spectrometer resolution. Both ends of the baseline were set sufficiently far apart so as not to distort the shape of spectra, including the tails. Small variations in the range of the baseline had no effect on the relative amount of fitted species (less than 1%). As we reported previously, all binding energies were calibrated by referencing Au $4f_{7/2}$ (84.0 eV) and Cu $2p_{3/2}$ (932.66 eV) of sputter-cleaned Au and Cu.[17,18] For homogeneous alloys of Pt and Ni, a simple linear expression furnished quantitative results. We either experimentally measured the pure element intensities (e.g., pure Pt and a thick layer of Ni on Pt) or used sensitivity factors for Pt 4f and Ni 2p from the literature.[19,20] This simple relationship permits estimations of the number of monolayers but not the surface coverage.

Electrochemical measurements were investigated using a three-electrode cell at room temperature.[7,8] The prepared thin-film electrodes were used as a working electrode. Pt wire and Ag/AgCl (in saturated KCl) were used as a counter and a reference electrode, respectively. Electrochemical characteristic curves in 2 M CH_3OH + 0.5 M H_2SO_4, which were stirred constantly and purged with nitrogen gas, were recorded with an Eco Chemie (Netherlands) AUTOLAB. All chemicals used were of analytical grade.

Results and Discussion

Structural Analysis of Pt/Ni Thin-Film Electrodes by X-ray Diffraction and Auger Electron Spectroscopy. The X-ray diffraction (XRD) peak shift of Pt and Ni with respect to annealing temperature is shown in Figure 1, compared with that of the as-deposited Pt/Ni thin-film electrode. The (111) peaks of Pt and Ni of the as-deposited electrode without any heat treatment are located at 39.7 and 44.5°, respectively, having the original peak positions of their metallic states. As the annealing temperature of the thin-film layers was increased, the XRD peaks were shifted from the original position, forming a solid solution between the metals. The (111) peak of Pt was shifted to higher angles while that of Ni was shifted to lower angles compared with the original peak positions. Assuming alloy formation between Pt and Ni based on a substitutional solid solution, such a shift in Figure 1 is due to the difference in size between Pt and Ni atoms. In Table 1, the compositions of Pt and Ni are compared with respect to annealing temperature upon the basis of Vegard's law using the equation below:

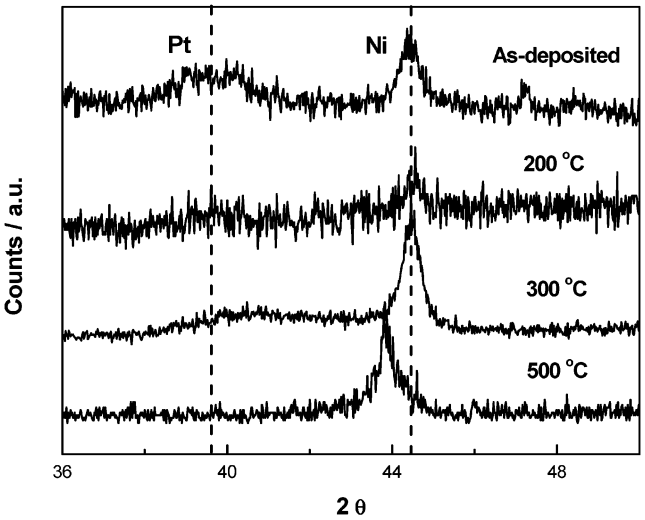

Figure 1. X-ray diffraction patterns of Pt/Ni thin-film electrodes as-deposited and annealed at 200, 300, and 500 °C followed by e-beam evaporation of a Pt and Ni metal layer.

TABLE 1: X-ray Diffraction Analysis of Pt/Ni Thin-Film Electrodes Annealed by a Rapid Thermal Annealing System Followed by Metal Film Deposition by an e-Beam Evaporator

annealing temp	Pt/Ni alloy electrode
as-deposited	no alloy formation
200 °C	$Pt_{95}Ni_5$
300 °C	$Pt_{58}Ni_{42}$
500 °C	$Pt_{13}Ni_{87}$

$$d_{PtNi} = Xd_{Pt} + (1 - X)d_{Ni}$$

where X is the composition of Pt in the Pt/Ni electrode and d_{PtNi}, d_{Pt}, and d_{Ni} are the d spacings of the (111) planes of PtNi, Pt, and Ni, respectively. The as-deposited Pt/Ni electrode shows no alloy formation. The Pt/Ni electrode annealed at 200 °C (200 °C Pt/Ni) mainly consists of a dominant Pt (95 at %) metallic phase. However, the Pt/Ni electrode annealed at 300 °C (300 °C Pt/Ni) contains 58 and 42 at % Pt and Ni, respectively, indicating that 300 °C Pt/Ni produces a Pt-based alloy electrode. The Pt/Ni electrode annealed at 500 °C (500 °C Pt/Ni) consists of 13 and 87 at % of Pt and Ni, respectively, indicating that 500 °C Pt/Ni produces a Ni-based alloy electrode. In addition, it is surprising that, in the XRD peaks of Pt/Ni electrodes, except for the metallic peak of Pt and Ni, no oxide peaks such as Pt oxides (PtO and PtO_2) and Ni oxides (NiO, NiOOH, and $Ni(OH)_2$) are apparent. However, from Auger electron spectroscopy and X-ray photoelectron spectroscopy (XPS) (see below), oxygen species are present in the Pt/Ni electrodes, and those are not crystalline oxidative states but surface and subsurface oxidative states.

To identify the elemental composition in the surface region and to analyze the interface composition, Auger electron spectra

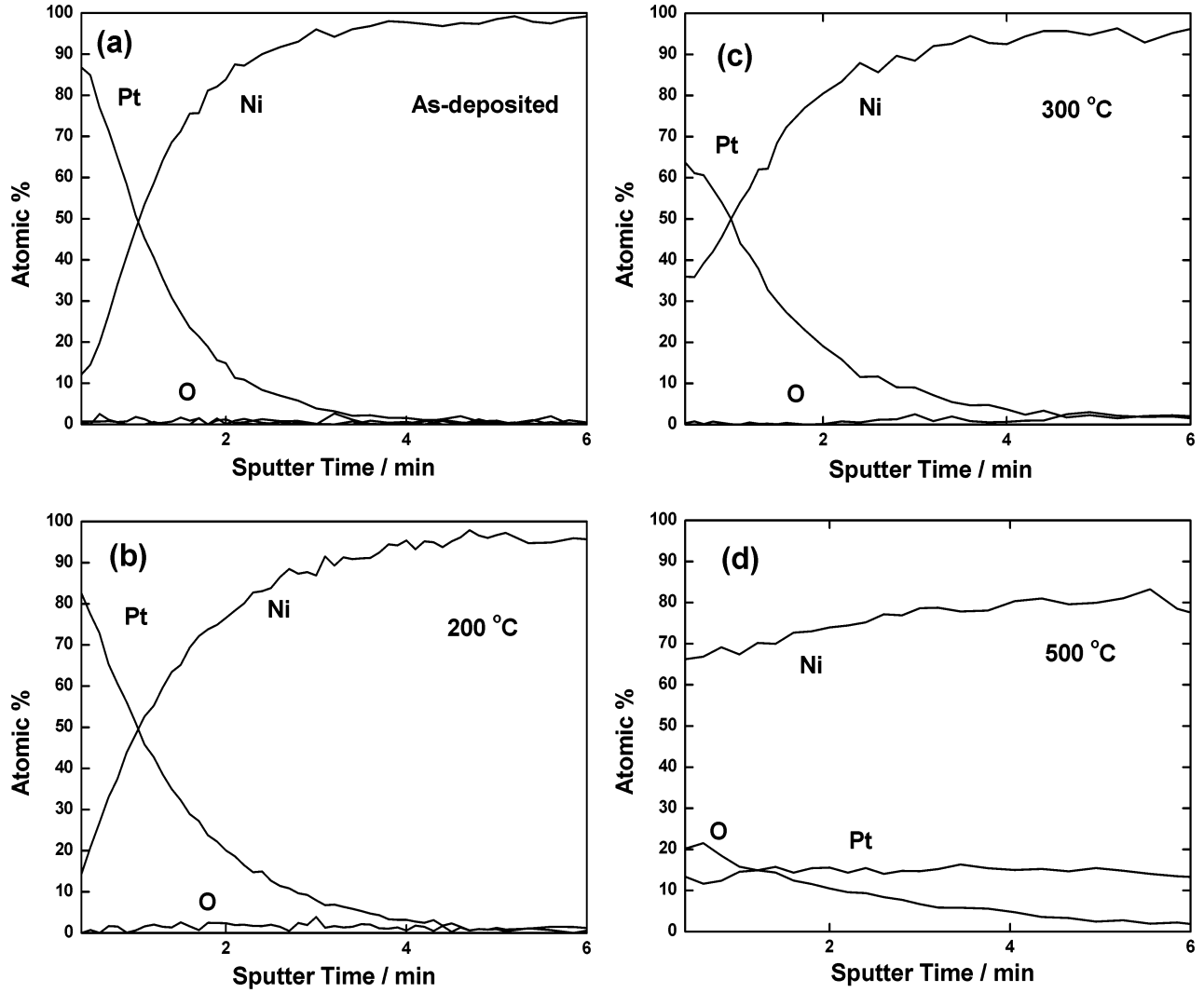

Figure 2. Auger electron spectra of Pt/Ni thin-film electrodes annealed at 200, 300, and 500 °C compared with that of an as-deposited thin-film electrode.

of the Pt/Ni electrodes with respect to annealing temperatures were obtained, as shown in Figure 2. The AES analysis is the most widely used analytical technique for obtaining the chemical composition of a solid surface. The main advantage of the analysis is its high sensitivity in the 5−20 Å region near the surface. In addition, it can be combined with ion-beam sputtering to remove the surface of a metal film and to continue to monitor the chemical composition of the remaining surface as this surface moves into the sample. As expected in the XRD of Figure 1, the annealing process results in intermixing states with elevating temperatures as the result of interdiffusion between the two thin metal films of Pt and Ni. In the case of the as-deposited electrode in Figure 2a and 200 °C Pt/Ni in Figure 2b, the surface layer of a few nanometers mainly consists of Pt. However, as the sputter time for depth profiling of the electrodes increases, a Ni layer appears followed by a Pt layer. The Pt phase in the 300 °C Pt/Ni (Figure 2c) is dominant compared to the Ni phase. In the case of Pt/Ni, the catalytic properties of the Pt surface of this alloy may be different from the properties of pure Pt due to intermetallic bonding with Ni in the surface layer below. It has been reported that Pt/Ni alloys provide a useful test of the so-called electronic factor in alloy electrocatalysis. Table 2 shows the atomic composition (at %) of elements at the surface and 2 nm in depth in order to compare the surface composition by XPS and the atomic composition by XRD, respectively. In

TABLE 2: Atomic Percent of Elements in Pt/Ni Thin-Film Electrodes, As Determined by Auger Electron Spectra at the Surface and a Depth of 2 nm

	atomic % at surface			atomic % at 2 nm depth		
annealing temp	Pt	Ni	O	Pt	Ni	O
as-deposited	86.9	12.1	1.2	77.0	19.8	3.2
200 °C	82.6	14.3	3.1	73.0	26.0	1.0
300 °C	63.7	35.9	0.4	61.0	36.0	3.0
500 °C	13.3	66.2	20.5	12.0	67.0	23.0

Table 2, the composition of the 200 °C Pt/Ni electrode is a Pt-dominant layer of 82.6 and 73.0 at % Pt at the surface and at the depth 2 nm, respectively. It is likely that the smaller portion (73.0 at %) of Pt measured at the depth 2 nm versus the 95 at % obtained by XRD results from elemental Ni which is intermixed with the Pt layer but does not participate in alloy formation. The composition at the surface is in agreement with values obtained by XPS analysis (see Table 3). The 300 °C Pt/Ni contains 35.9 and 37.0 at % Ni at the surface and at the depth 2 nm, which are similar to XPS and XRD data, respectively. As already described in the XRD of the 300 °C Pt/Ni, the composition of Ni, as calculated by Vegard's law, was approximately 42 at %. In the case of the 500 °C Pt/Ni electrode (Figure 2d and Table 2), the composition of a Pt/Ni thin film is interchanged into a Ni-dominant layer of 86 at %

TABLE 3: Composition of Pt/Ni Thin-Film Electrodes by X-ray Photoelectron Spectra

annealing temp	Pt (at %)	Ni (at %)
as-deposited	90.1	9.9
200 °C	82.5	17.5
300 °C	67.0	33.0
500 °C	23.9	76.1

at the depth 2 nm, consistent with the 87 at % Ni measured by XRD. Considering the AES and XRD data for the 300 and 500 °C Pt/Ni, all the Ni, intermixed into the Pt layer in the electrodes, could be joined by alloy formation between Pt and Ni, in contrast to the case of the electrode annealed at 200 °C (200 °C Pt/Ni). Alloy formation of the Pt/Ni electrode as the result of the incorporation of all the Ni would lead to a modification in the chemical and electronic properties of the thin-film catalyst, as will seen in the section below on XPS analysis, as well as structural changes observed by XRD and AES analysis.

Combining thin film electrode structure as evidenced by XRD and AES data, according to the annealing temperature of e-beam evaporated film layers, the Pt/Ni electrodes can be classified into three types: Pt-dominant (as-Pt/Ni or 200 °C Pt/Ni), Pt-based (300 °C Pt/Ni), and Ni-dominant (500 °C Pt/Ni). The three types of electrodes can be comparable to synthesized nanoparticles of any composition, and the mechanism and their effect on methanol electrooxidation is discussed below. Gauthier et al.[21] reported on the surface structure and near-surface structure of $Pt_{50}Ni_{50}$ and $Pt_{78}Ni_{22}$ single crystals using low-energy electron diffraction (LEED) crystallography and low-energy ion scattering (LEIS). They found, despite the identical surface energies of Pt and Ni, a strong enrichment of the surface in Pt, in agreement with our AES and XPS data. The well-defined alloy thin-film electrodes play a significant role in the development of chemical and electronic models for electrocatalysis in polycrystalline samples. In particular, since the average particle size of Pt/Ni alloy nanoparticles synthesized in this work is less than 4 nm, the entire bulk composition can only be guessed from an escape depth of about 2−3 nm of the photoelectrons of the XPS scrutiny. However, in the case of thin-film electrodes, the correlation and compensation of depth profiling by AES with surface analysis by XPS enable us to better understand the alloy nanostructure and to confirm any effects.

Chemical and Electronic Properties of Pt/Ni Thin-Film Electrodes by X-ray Photoelectron Spectroscopy. Figure 3 shows Ni 2p spectra of thin-film electrodes with respect to annealing temperatures. In the Ni 2p spectra, the as-deposited electrode showed no Ni peaks at the surface layer because of the presence of a Pt layer a few nanometers thick and the transmission limit of the XPS beam. However, as the annealing temperature is increased, surface Ni metallic and oxidative states begin to appear. The 300 °C Pt/Ni mainly contains metallic Ni-(Ni^0) and a hydroxide form while 500 °C Pt/Ni contains metallic Ni(Ni^0) and dominant surface oxidative states. In general, the Ni 2p spectrum has a complex structure with intense satellite signals of high binding energy adjacent to the main peaks, which can be attributed to multielectron excitation. After these shake-up peaks are considered, the Ni 2p XPS peaks (Figure 3a) of 300 °C Pt/Ni at binding energies of 852.7 and 855.6 eV correspond to Ni° and $Ni(OH)_2$. The Ni 2p spectra (Figure 3b) for 500 °C Pt/Ni indicate the presence of Ni°, NiO, and Ni-$(OH)_2$. Table 3 shows the composition of Pt/Ni thin-film electrodes, as confirmed by XPS spectra. The surface composition of Ni in 200 °C Pt/Ni, 300 °C Pt/Ni, and 500 °C Pt/Ni is 17.5, 33.0, and 66.1 at %, respectively. However, the portion

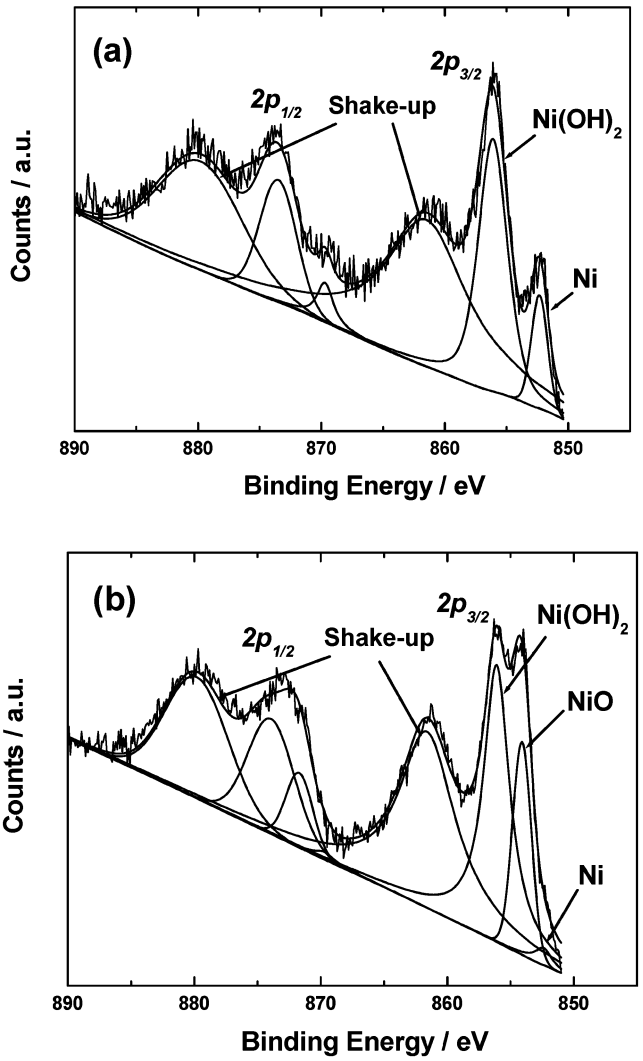

Figure 3. Ni 2p peaks of X-ray photoelectron spectra of Pt/Ni thin-film electrodes annealed at (a) 300 °C and (b) 500 °C.

of Ni based upon AES analysis is higher than that based on XPS. This supports the conclusion that, although the heats of vaporization of Pt and Ni are 509.6 and 370.3 kJ/mol, respectively, Pt is enriched on the surface.[7] In particular, it has recently been reported that nickel or nickel hydroxides acting as a catalyst are capable of oxidizing methanol in alkaline or acid solution. Kowal et al.[22] and El-Shafei[23] reported a nickel hydroxide such as $Ni(OH)_2$ on the nickel metal electrode for methanol oxidation in alkaline solutions. The Ni hydroxide layer has some other favorable properties, such as proton and electronic conductivity, and is well protected from corrosion under conditions of methanol oxidation. Such a hydroxide layer on the Pt/Ni electrodes may display a high catalytic activity with respect to methanol oxidation.

Pt 4f XPS spectra for Pt/Ni thin-films are shown in Figure 4 and Table 4, which is compared to a spectrum obtained for pure Pt. The interesting point in the Pt XPS spectra is that the Pt 4f peaks of the annealed electrodes are shifted to a lower binding energy than that of the original peak position (as-deposited), as shown in Figure 4. The peaks are shifted from 0.1 eV for 200 °C Pt/Ni to 0.6 eV for 300 °C Pt/Ni and 0.4 eV for 500 °C Pt/Ni, moving toward the lower Pt 4f binding energy. In the structural analysis such as alloy formation and intermixing effects using XRD and AES, all the Ni in the 300 and 500 °C Pt/Ni appears to participate in alloy formation, while most of

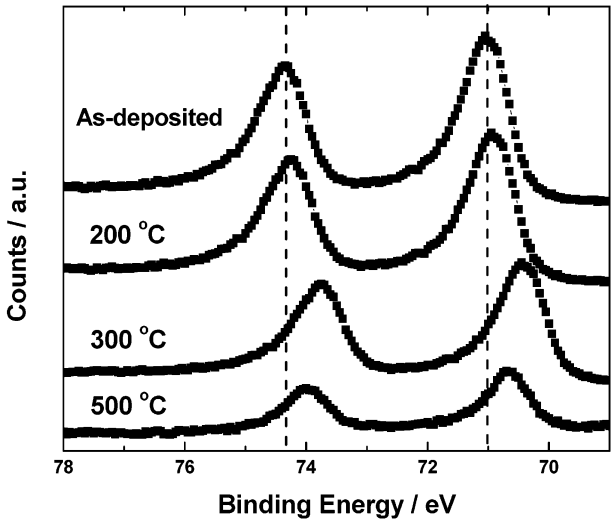

Figure 4. Pt 4f peaks of X-ray photoelectron spectra of Pt/Ni thin-film electrodes. The dashed line indicates the Pt 4f peak of a pure Pt thin-film deposited by e-beam evaporation.

TABLE 4: Pt 4f Peaks of X-ray Photoelectron Spectra in Pt/Ni Thin-Film Electrodes

	Pt 4f	
annealing temp	$4f_{7/2}$	$4f_{5/2}$
as-deposited	71.0	74.3
200 °C	70.9	74.2
300 °C	70.4	73.7
500 °C	70.6	73.9

the elemental Ni in the 200 °C Pt/Ni was not alloyed with the Pt matrix. As described above, it would be expected that alloy formation of a Pt/Ni electrode with the Ni would lead to a modification in the electronic properties of the thin-film catalyst, the Pt 4f peak shift in the XPS. Accordingly, in the case of well-alloyed Pt/Ni electrodes, the 300 and 500 °C Pt/Ni show larger XPS peak shifts to low binding energy compared to case of the less-alloyed 200 °C Pt/Ni. In particular, the 300 °C Pt/Ni, the Pt-based alloy catalyst containing ~40 at % Ni, shows the largest modified electronic properties of Pt. Such a negative binding energy shift is responsible for an electron donation of Ni to Pt resulting in a change in the electronic properties of the Pt 4f peaks as a function of annealing temperature. The findings herein indicate that the modified electronic properties of platinum improved the electrocatalytic activity of Pt/Ni alloys, as evidenced by the electrochemical measurements below. The shift in d electron density from Ni to Pt would lower the density of state (DOS) on the Fermi level and reduce the Pt−CO bond energy,[24,25] as has been confirmed for Pt/Ni nanoparticles.[7]

Electrochemical Properties of Pt/Ni Thin-Film Electrodes and Pt/Ni-Based Alloy Nanoparticles for Methanol Electrooxidation. Figure 5 shows a plot of current density versus applied potential of Pt/Ni thin-film electrodes for methanol electrooxidation. The 300 °C Pt/Ni shows superior current density compared to those of the as-deposited, 200 °C, and 500 °C Pt/Ni. This indicates that a Pt/Ni thin-film electrode deposited in the form of layer (Ni) by layer (Pt) has an optimum annealing temperature for achieving a high catalytic activity. It is probable that the low catalytic activity of the 200 °C Pt/Ni is responsible for the absence of an electronic effect and low alloy formation. However, a considerable amount of Ni is involved in the surface layer structure, reducing the active sites of Pt, based on the XRD and AES results. The 500 °C Pt/Ni also shows a low methanol electrooxidation current density due to Ni-based alloy formation,

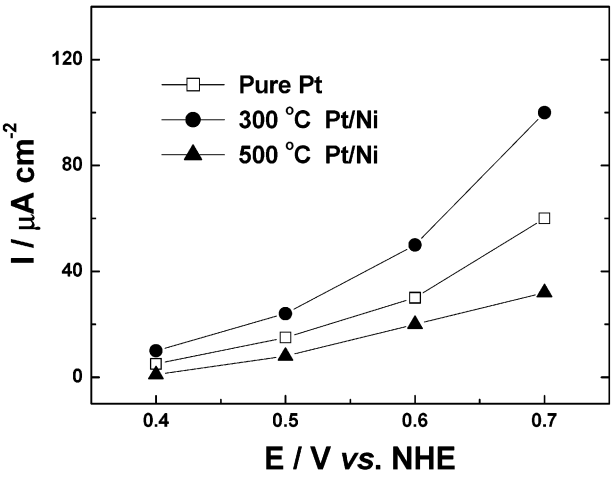

Figure 5. Plot of methanol electrooxidation current density vs potential for Pt/Ni thin-film electrodes in 2 M CH_3OH + 0.5 M H_2SO_4.

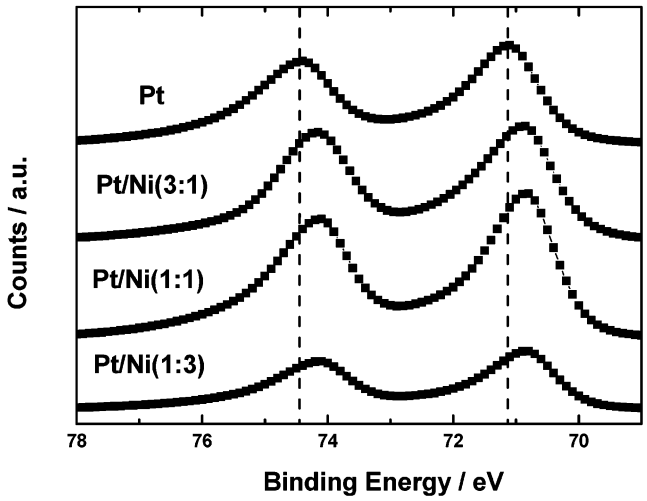

Figure 6. Pt 4f peaks of X-ray photoelectron spectra in Pt/Ni nanoparticles. The dashed line indicates the Pt 4f peak of pure Pt nanoparticles synthesized by borohydride reduction.

that is, a Ni-dominant surface layer, even if an electronic effect exists. On the other hand, the 300 °C Pt/Ni has the best performance in terms of methanol electrooxidation. The enhanced activity of the 300 °C Pt/Ni can be attributed to optimized Pt-based alloy formation and an electronic effect, that is, a modification of electronic properties in Pt 4f. Electron transfer from Ni to Pt can be explained by the electronegativities of Ni and Pt: 1.91 and 2.28. The shift in d electron density from Ni to Pt would be expected to lower the DOS on the Fermi level and to reduce the bond energy of Pt and CO as a byproduct of methanol electrooxidation. While an electronic interpretation of the catalytic enhancement results is quite tempting, it has already been pointed out that Ni (hydro)oxides on the Pt/Ni nanoparticles could promote methanol oxidation via a surface redox process. These two contributions to enhancing methanol electrooxidation would exist in the Pt/Ni based electrodes.

Figures 6 and 7 show that the modified electronic properties in the Pt/Ni nanoparticles are closely related to their catalytic activities for methanol electrooxidation. The Pt 4f XPS peaks of the Pt/Ni nanoparticles are shifted from −0.35 eV for Pt/Ni(1:1) and −0.36 eV for Pt/Ni(3:1), as shown in Figure 6. It has been reported that Pt/Ni alloy nanoparticles provide evidence for a change in the electronic structure of Pt when it is alloyed with Ni. Using Pt/Ni nanoparticles, plots of methanol oxidation current versus potential were measured in 2 M CH_3OH + 0.5

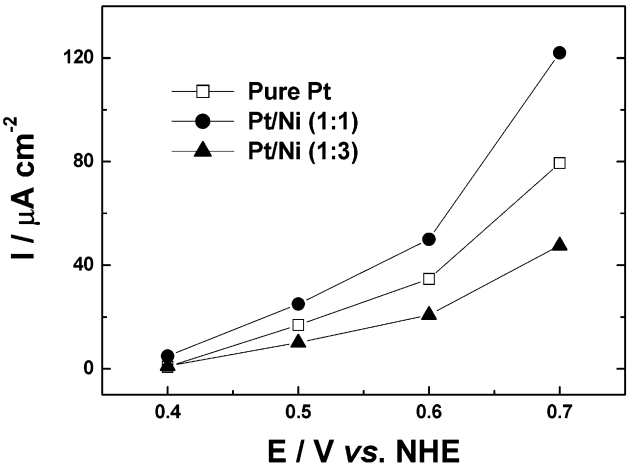

Figure 7. Plot of methanol electrooxidation current vs potential in 2 M CH_3OH + 0.5 M H_2SO_4 for Pt/Ni nanoparticles synthesized by borohydride reduction.

M H_2SO_4, as shown in Figure 7. Pt/Ni(1:1) nanoparticles support a higher current and thus have a higher catalytic activity than pure Pt. However, a Ni-based electrode such as Pt/Ni(1:3) shows less catalytic activity than Pt. The situation for the Pt/Ni nanoparticles is in good agreement with that for Pt/Ni thin films. As shown in Figure 5, the 300 °C Pt/Ni electrode is superior to the other electrodes. The 300 °C Pt/Ni electrode has properties by XRD and XPS corresponding to Pt/Ni(1:1), that is, a Pt-based alloy structure and modified electronic properties in Pt 4f. On the other hand, the electrode with an electronic effect but having a Ni-based structure such as 500 °C Pt/Ni, similar to Pt/Ni(1:3), has a low catalytic activity for methanol electrooxidation. In effect, the Pt/Ni(1:1) nanoparticles synthesized by borohydride reduction[7,26,27] show a composition of $Pt_{60}Ni_{40}$, as evidenced by XRD analysis with a surface composition of 53.4 and 46.6 at % Pt and Ni, respectively. On the other hand, the 300 °C Pt/Ni thin-film electrode contained $Pt_{58}Ni_{42}$ by XRD structural analysis with 63.0 at % Pt and 37.0 at % Ni by AES at a depth of 2 nm and 67.0 at % Pt and 33.0 at % Ni by XPS. This indicates that the Pt/Ni thin-film electrodes can be compared with Pt/Ni nanoparticles of various compositions synthesized by the chemical method in terms of structural, chemical, and electronic properties. Accordingly, thin-film electrodes fabricated using an e-beam evaporator and RTA would lead to active catalysis on the alloy surface layer. However, for a complete understanding and modeling of alloy catalysts, a systematic experimental process for the fabrication of thin-film electrodes in the electrocatalysis will be required.

Conclusions

Thin-film electrodes were fabricated by e-beam evaporation of metal layers and RTA to achieve alloy formation between the Pt and Ni layers. Depending on the annealing temperatures of 200, 300, and 500 °C used in the RTA system, the structural, chemical, and electronic properties of the thin-film electrodes were characterized by classifying them into three-types of Pt/Ni catalysts: Pt-dominant (as-Pt/Ni or 200 °C Pt/Ni), Pt-based (300 °C Pt/Ni), and Ni-dominant (500 °C Pt/Ni). The Pt/Ni thin-film electrodes were compared and were comparable to Pt/Ni nanoparticles synthesized in a variety of compositions: Pt-dominant (Pt/Ni(3:1)), Pt-based (Pt/Ni(1:1)), and Ni-dominant (Pt/Ni(1:3)). Among the Pt/Ni catalysts, the Pt-based alloy structure showed the highest catalytic activity in methanol electrooxidation and the largest shift in the Pt 4f peak in the XPS. The modified electronic properties of platinum in the Pt/Ni alloy catalysts can be attributed to the Pt-based surface and a bulk structure such as the 300 °C Pt/Ni thin-film electrode and Pt/Ni(1:1) nanoparticles, systematically matching the film and nanoparticle system. Therefore, we strongly suggest that thin-film electrodes fabricated by e-beam evaporation and RTA processing can be used in the systematic modeling of alloy nanoparticles for use in electrocatalysis in direct methanol fuel cells or directly applied to thin-film fuel cells.

Acknowledgment. This work was supported by Korea Research Foundation Grant KRF-2002-041-D00153.

References and Notes

(1) Hearth, M. P.; Hards, G. A. *Platinum Met. Rev.* **1996**, *40*, 150.
(2) Oetjen, H.-F.; Schmidt, V. M.; Stimming, U.; Trila, F. *J. Electrochem. Soc.* **1996**, *143*, 3838.
(3) Hamnett, A. *Catal. Today* **1997**, *38*, 445.
(4) Reddington, E.; Sapienza, A.; Gurau, B.; Viswanathan, R.; Sarangapani, S.; Smotkin, E. S.; Mallouk, T. E. *Science* **1998**, *280*, 1735.
(5) Ross, P. N. In *Electrocatalysis*; Lipkowski, J., Ross, P. N., Eds.; Wiley-VCH: New York, 1998; Chapter 2.
(6) Wieckowski, A., Ed. In *Interfacial Electrochemistry*; Marcel-Dekker: New York, 1999; Chapter 44−51.
(7) Park, K.-W.; Choi, J.-H.; Kwon, B.-K.; Lee, S.-A.; Sung, Y.-E.; Ha, H.-Y.; Hong, S.-A.; Kim, H.; Wieckowski, A. *J. Phys. Chem. B* **2002**, *106*, 1869.
(8) Lee, S.-A.; Park, K.-W.; Choi, J.-H.; Kwon, B.-K.; Sung, Y.-E. *J. Electrochem. Soc.* **2002**, *149*, 1299.
(9) Park, K.-W.; Ahn, K.-S.; Choi, J.-H.; Nah, Y.-C.; Kim, Y.-M.; Sung, Y.-E. *Appl. Phys. Lett.* **2002**, *81*, 907.
(10) Herrero, E.; Franaszczuk, K.; Wieckowski, A. *J. Phys. Chem. B* **1994**, *98*, 5074.
(11) Watanabe, M.; Motoo, S. *J. Electroanal. Chem.* **1975**, *60*, 275.
(12) Liu, R.; Iddir, H.; Fan, Q.; Hou, G.; Bo, A.; Ley, K. L.; Smotkin, E. S.; Sung, Y.-E.; Kim, H.; Thomas, S.; Wieckowski, A. *J. Phys. Chem. B* **2000**, *104*, 3518.
(13) Goodenough, J. B.; Manoharan, R.; Shukla, A. K.; Ramesh, K. V. *Chem. Mater.* **1989**, *1*, 391.
(14) Toda, T.; Igarashi, H.; Uchida, H.; Watanabe, M. *J. Electrochem. Soc.* **1999**, *146*, 3750.
(15) Rodriguez, J. A.; Goodman, D. W. *Science* **1992**, *257*, 897.
(16) Jinang, X.; Permeter, J. E.; Estrada, C. A.; Goodman, D. W. *Surf. Sci.* **1991**, *249*, 44.
(17) Sherwood, P. M. A. In *Practical Surface Analysis*; Briggs, D., Seah, M. P., Eds.; Wiley: New York, 1990; Appendix 3.
(18) Moulder, J. F.; Stickle, W. F.; Sobol, P. E.; Bomben, K. D. In *Handbook of X-ray Photoelectron Spectroscopy*; Chastin, J., Ed.; Physical Electronics: Eden Prairie, MN, 1992.
(19) Wagner, C. D.; Davis, L. E.; Zeller, M. V.; Taylor, J. A.; Raymond, R. M.; Gale, L. H. *Surf. Interface Anal.* **1981**, *3*, 211.
(20) Chan, R. W. M.; Kwok, R. W. M.; Lau, W. M.; Yan, H.; Wong, S. P. *J. Vac. Sci. Technol., A* **1997**, *15*, 2787.
(21) Gauthier, Y.; Joly, Y.; Baudoing, R.; Rundgren, J. *Phys. Rev. B* **1985**, *31*, 6216.
(22) Kowal, A.; Port, S. N.; Nichols, R. J. *Catal. Today* **1997**, *38*, 483.
(23) El-Shafei, A. A. *J. Electroanal. Chem.* **1999**, *471*, 89.
(24) Tong, Y. Y.; Kim, H. S.; Babu, P. K.; Waszczuk, P.; Wieckowski, A.; Oldfield, E. *J. Am. Chem. Soc.*, submitted.
(25) Ishikawa, Y.; Liao, M. S.; Cabrera, C. R. *Surf. Sci.* **2000**, *463*, 66.
(26) Kinoshita, K.; Stonehart, P. *Modern Aspect of Electrochemisty*; Plenum Press: New York, 1996; p 12.
(27) Klabunde, K. J.; Mohs, C. In *Chemistry of Advance Materials*; Interrante, L. V., Hampden-Smith, L. V., Eds.; Wiley-VCH: New York, 1998; Chapter 3.